Comput. Methods Appl. Mech. Engrg. 198 (2009) 3105–3112

Contents lists available at ScienceDirect

Comput. Methods Appl. Mech. Engrg.

journal homepage: www.elsevier.com/locate/cma

A generalized continuous surface tension force formulation for phase-field models for multi-component immiscible fluid flows

Junseok Kim *

Department of Mathematics, Korea University, Seoul 136-701, Republic of Korea

ARTICLE INFO

Article history:
Received 11 December 2008
Received in revised form 10 May 2009
Accepted 14 May 2009
Available online 21 May 2009

Keywords:
Continuum surface tension
Phase-field model
Navier–Stokes equation
Multi-component Cahn–Hilliard equation
Interfacial tension
Nonlinear multigrid method

ABSTRACT

We present a new phase-field method for modeling surface tension effects on multi-component immiscible fluid flows. Interfaces between fluids having different properties are represented as transition regions of finite thickness across which the phase-field varies continuously. At each point in the transition region, we define a force density which is proportional to the curvature of the interface times a smoothed Dirac delta function. We consider a vector valued phase-field, the velocity, and pressure fields which are governed by multi-component advective Cahn–Hilliard and modified Navier–Stokes equations. The new formulation makes it possible to model any combination of interfaces without any additional decision criteria. It is general, therefore it can be applied to any number of fluid components. We give computational results for the four component fluid flows to illustrate the properties of the method. The capabilities of the method are computationally demonstrated with phase separations via a spinodal decomposition in a four-component mixture, pressure field distribution for three stationary drops, and the dynamics of two droplets inside another drop embedded in the ambient liquid.

1. Introduction

The interfacial hydrodynamics of a mixture of different fluids plays an increasingly important role in many current scientific and bio-medical engineering applications [15,25,27]. Examples include extractors, separators, reactors, sprays, polymer blends, and microfluidic technology [26,27]. A fluid–fluid interface is in a state of tension, as though interfaces have an elastic skin, because fluid molecules at or near the interface experience uneven molecular forces of attraction [28]. Due to the inherent nonlinearities, topological changes, and the complexity of dealing with the unknown, active, and moving surfaces, multiphase flows are challenging. Much effort has been put into studying such flows through analysis, asymptotics, and numerical simulation.

There are many ways to characterize and model moving interfaces. The two main approaches to simulating multiphase and multicomponent flows are interface tracking and interface capturing. In interface tracking methods (examples include volume-of-fluid [14,31], which tracks the volume of the fluid in each cell; front-tracking [38], immersed boundary [39], and immersed interface [24]), Lagrangian (or semi-Lagrangian) particles are used to track the interfaces. In interface capturing methods such as level-set [5,29,34,35] and phase-field methods [6,18,40], the interface is implicitly captured by a contour of a particular scalar function (for example, a signed distance function in a level-set method and mass concentration in a phase-field method). Readers can review a recent review paper [22] for details of the two-phase flow models.

However, compared to the large body of research on two-phase [2,5,6,11,14,32,33,37] and three-phase [3,19,21,36] fluid flows, there have been few theoretical and numerical studies of flows containing four (or more) liquid components with a surface tension effect. The basic idea underlying all continuum surface tension models is the representation of surface tension as a continuous force per unit volume that acts in a neighborhood of the interface. Previous methods have suffered, however, from difficulties in modeling more than three component fluid flows with surface tension. One of the greatest difficulties in modeling four immiscible fluid flows is modeling surface tension effects.

In three component fluids [3,19,21,36], the phase specific decomposition surface forces are used. We decompose the given physical surface tension coefficients, σ_{ij}, of the interface Γ_{ij} between fluid $i(\Omega_i)$ and fluid $j(\Omega_j)$ (see Fig. 1a) into the phase specific surface tension coefficients σ_1, σ_2, and σ_3 such that:

$$\sigma_{12} = \sigma_1 + \sigma_2, \quad \sigma_{13} = \sigma_1 + \sigma_3, \quad \sigma_{23} = \sigma_2 + \sigma_3. \tag{1}$$

The decomposition is uniquely defined as $\sigma_1 = (\sigma_{12} - \sigma_{23} + \sigma_{13})/2$, $\sigma_2 = (\sigma_{12} + \sigma_{23} - \sigma_{13})/2$, and $\sigma_3 = (-\sigma_{12} + \sigma_{23} + \sigma_{13})/2$ (see Fig. 1b–d). Then the continuous surface tension force is defined as

* Tel.: +82 2 3290 3077; fax: +82 2 929 8562.
E-mail address: cfdkim@korea.ac.kr

0045-7825/$ - see front matter © 2009 Elsevier B.V. All rights reserved.
doi:10.1016/j.cma.2009.05.008

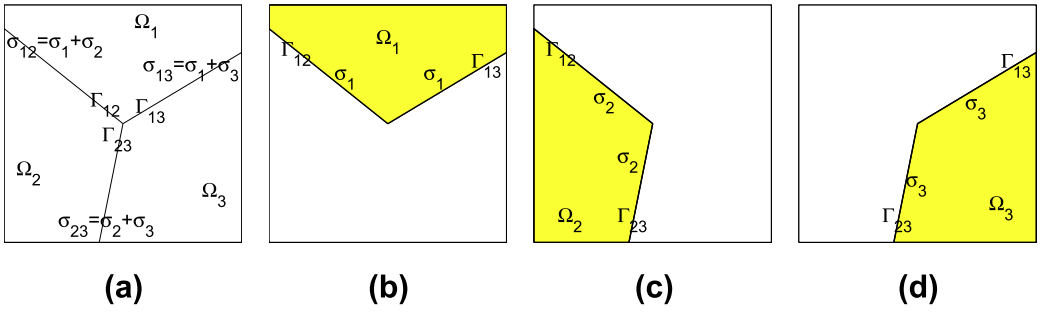

Fig. 1. Schematic of domain. (a) σ_{ij} denotes the surface tension coefficient of the interface Γ_{ij} of fluids Ω_i and Ω_j. (b) Phase specific surface tension coefficient, σ_1, on interfaces, Γ_{12} and Γ_{13}. (c) and (d) are similarly defined.

$$\mathbf{SF} = \sum_{k=1}^{3} \mathbf{SF}_k = \sum_{k=1}^{3} \sigma_k \kappa(c_k)\mathbf{n}(c_k)\delta(c_k), \tag{2}$$

where $\kappa(c_k) = \nabla \cdot (\nabla c_k/|\nabla c_k|)$, $\mathbf{n}(c_k)$, and $\delta(c_k)$ are the mean curvature, the unit normal vector, and the smoothed Dirac delta function of the k-th fluid interface, respectively. c_k is the phase variable to be defined.

It has been noted by several authors [3,21] that in the quaternary case, the use of phase specific decomposition cannot be used. This is because the decomposition generates a system of over-determined equations and a solution may not exist. In fact, in [36], "$n > 2$" only means "$n = 3$". Here n represents the number of fluid components. For example, if $n = 4$, then given the physical surface tension coefficients σ_{ij} of the interface Γ_{ij} between fluid i and fluid j, we may consider a linear system of six equations to determine the four unknowns $\sigma_1, \sigma_2, \sigma_3$, and σ_4:

$$\begin{aligned} &\sigma_{12} = \sigma_1 + \sigma_2, \quad \sigma_{13} = \sigma_1 + \sigma_3, \quad \sigma_{14} = \sigma_1 + \sigma_4, \\ &\sigma_{23} = \sigma_2 + \sigma_3, \quad \sigma_{24} = \sigma_2 + \sigma_4, \quad \sigma_{34} = \sigma_3 + \sigma_4. \end{aligned} \tag{3}$$

But the above systems of equations are over-determined equations; therefore, it is possible that there is no solution. In order that these equations possess a unique solution, some restrictions must be imposed on σ_{ij}. Note that, in general, for n component immiscible fluid system there are $n(n-1)/2$ possible interfaces and $n(n-1)/2 > n$ for $n \geqslant 4$. This implies that we have more equations than the unknowns.

To the author's knowledge, there are no four (or more) component fluid flow continuum models with surface tension effects. The main objective of this work is to develop a generalized continuous surface tension force (GCSF) formulation for phase-field models for multi-component immiscible fluid flows, having no difficulty with the over-determined system problem. Phase-field methods have become popular tools for physical modeling of multiphase systems (for a review of the development of diffuse-interface models, see [1]). Generalizations of phase-field models to any number of components without hydrodynamic surface tension effects have been recently introduced and studied in [8,9,12,13,20]. Here, we view the phase-field model as a computational method. The proposed phase-field model is a hybrid method which combines a level set type surface tension force formulation and a concentration relaxation by a phase-field model.

The outline of the paper is as follows. In Section 2, we propose a phase-field model for four immiscible fluids. In Section 4, we perform some characteristic numerical experiments for quaternary fluid flows. In Section 5, conclusions are drawn.

2. A phase-field model for the mixture of four component immiscible fluids

2.1. Governing equations

The composition of a quaternary mixture (A, B, C, and D) can be mapped onto an equilateral tetrahedron (the Gibbs simplex [30]) whose corners represent a 100% concentration of A, B, C, or D as shown in Fig. 2a. Mixtures with components lying on planes parallel to the triangle, ΔBCD, contain the same percentage of A; those with planes parallel to the triangle, ΔCDA, have the same percentage of B concentration; analogously, for the C and the D concentrations. In Fig. 2, the mixture at the position marked '$\circ$' contains 20% A, 24% B, 48%C and 8% D.

Let $\mathbf{c} = (c_1, c_2, c_3, c_4)$ be the phase variables (i.e. the mole fractions of A, B, C, and D, respectively). Thus, admissible states will belong to the Gibbs tetrahedron

$$GT := \left\{ \mathbf{c} \in \mathbb{R}^4 \middle| \sum_{i=1}^{4} c_i = 1, 0 \leqslant c_i \leqslant 1 \right\}. \tag{4}$$

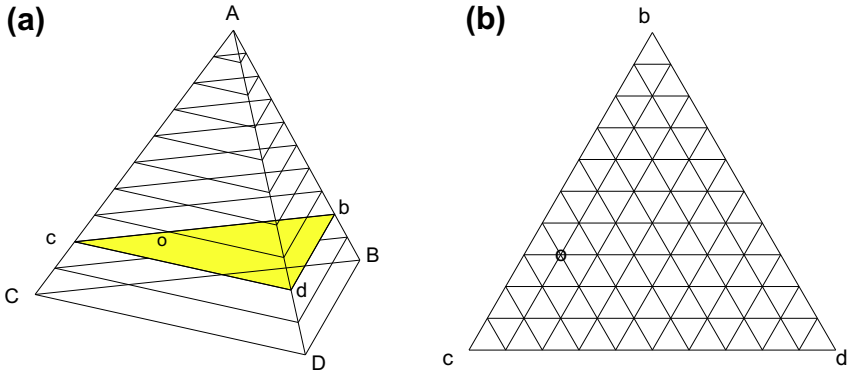

Fig. 2. (a) Gibbs tetrahedron. (b) A slice plane parallel to the *BCD* triangle.

Without loss of generalities, we postulate that the free energy can be written as follows

$$\mathscr{F} = \int_\Omega \left[F(\mathbf{c}) + \frac{\epsilon^2}{2} \sum_{i=1}^{4} |\nabla c_i|^2 \right] d\mathbf{x},$$

where $F(\mathbf{c}) = 0.25 \sum_{i=1}^{4} c_i^2 (1-c_i)^2$, ϵ is a positive constant, and Ω is an open bounded subset of $\mathbb{R}^n (n = 2, 3)$ occupied by the system. The time evolution of $\mathbf{c}$ is governed by the gradient of the energy with respect to the H^{-1} inner product under the additional constraint (4). This constraint has to hold everywhere at any time. In order to ensure this last constraint, we use a variable Lagrangian multiplier $\beta(\mathbf{c})$ [12]. The time dependence of c_i is given by the following advective Cahn–Hilliard equation for describing each phase convection:

$$\frac{\partial c_i}{\partial t} + \mathbf{u} \cdot \nabla c_i = M \Delta \mu_i, \quad i = 1, 2, 3, 4, \tag{5}$$

$$\mu_i = \frac{\partial F(\mathbf{c})}{\partial c_i} - \epsilon^2 \Delta c_i + \beta(\mathbf{c}), \tag{6}$$

where $\mathbf{u}$ is the fluid velocity and M is the mobility. To calculate $\beta(\mathbf{c})$, we write an equation satisfied by $S = c_1 + c_2 + c_3 + c_4$ and we want $S \equiv 1$ to be a solution to the following equation

$$\frac{\partial S}{\partial t} + \mathbf{u} \cdot \nabla S = M \Delta \left(\sum_{i=1}^{4} \frac{\partial F}{\partial c_i} - \epsilon^2 \Delta S + 4\beta(\mathbf{c}) \right),$$

where we got this from the summation of Eq. (5) from $i = 1$ to $i = 4$. Therefore, $\beta(\mathbf{c}) = -0.25 \sum_{i=1}^{4} \partial F / \partial c_i$. For the sake of simplicity, we consider a system of four immiscible fluids where the densities of all fluids are taken to be equal. The variable density can be defined as $\rho(\mathbf{c}) = \left(\sum_{i=1}^{4} c_i / \rho_i \right)^{-1}$ and ρ_i is the i-th fluid density [21]. The fluids are incompressible and are governed by the Navier–Stokes–Cahn–Hilliard equations [2,3,6,17–19,21,22].

$$\rho \left(\frac{\partial \mathbf{u}}{\partial t} + \mathbf{u} \cdot \nabla \mathbf{u} \right) = -\nabla p + \nabla \cdot [\eta(\mathbf{c})(\nabla \mathbf{u} + \nabla \mathbf{u}^T)] + \mathbf{SF}, \tag{7}$$

$$\nabla \cdot \mathbf{u} = 0, \tag{8}$$

$$\frac{\partial \mathbf{c}}{\partial t} + \mathbf{u} \cdot \nabla \mathbf{c} = M \Delta \boldsymbol{\mu}, \tag{9}$$

$$\boldsymbol{\mu} = \mathbf{f}(\mathbf{c}) - \epsilon^2 \Delta \mathbf{c}, \tag{10}$$

where p is the pressure, $\eta(\mathbf{c}) = \left(\sum_{i=1}^{4} c_i / \eta_i \right)^{-1}$ is the variable viscosity, $\mathbf{SF}$ is the surface tension force, and $\mathbf{f}(\mathbf{c}) = (\partial F / \partial c_1 + \beta(\mathbf{c}), \partial F / \partial c_2 + \beta(\mathbf{c}), \partial F / \partial c_3 + \beta(\mathbf{c}), \partial F / \partial c_4 + \beta(\mathbf{c}))$.

To avoid the solvability problem imposed by the over-determined system (3), we propose a generalized continuous surface tension force formulation:

$$\begin{aligned} \mathbf{SF}(\mathbf{c}) = {} & \frac{\sigma_{12}}{2} [\mathbf{sf}(c_1) + \mathbf{sf}(c_2)] \delta(c_1, c_2) + \frac{\sigma_{13}}{2} [\mathbf{sf}(c_1) \\ & + \mathbf{sf}(c_3)] \delta(c_1, c_3) + \frac{\sigma_{14}}{2} [\mathbf{sf}(c_1) + \mathbf{sf}(c_4)] \delta(c_1, c_4) + \frac{\sigma_{23}}{2} \\ & \times [\mathbf{sf}(c_2) + \mathbf{sf}(c_3)] \delta(c_2, c_3) + \frac{\sigma_{24}}{2} [\mathbf{sf}(c_2) \\ & + \mathbf{sf}(c_4)] \delta(c_2, c_4) + \frac{\sigma_{34}}{2} [\mathbf{sf}(c_3) + \mathbf{sf}(c_4)] \delta(c_3, c_4), \end{aligned} \tag{11}$$

where $\mathbf{sf}(c_i) = -\alpha \epsilon \nabla \cdot (\nabla c_i / |\nabla c_i|) |\nabla c_i| \nabla c_i$ and $\delta(c_i, c_j) = 5 c_i c_j$. The critical feature in the proposed surface tension force is incorporating a $\delta(c_i, c_j)$ function, which is the simplest form and combines two different fluids. Since we are using the chemical potential form, Eq. (6), we have $c_i \approx 1 - c_j$ at the interface, Γ_{ij}. For example, let us consider an initial configuration as shown in the Fig. 3a. From the darkest to the lightest region, the values of c_1, c_2, c_3, and c_4 are one, respectively. The Fig. 3b shows the vertical cutline of phase fields at $y = 0.5$ when the system reaches an equilibrium state. In this figure, $c_1 \approx 1 - c_2, c_2 \approx 1 - c_3$, and $c_3 \approx 1 - c_4$ at the interfaces, Γ_{12}, Γ_{23}, and Γ_{34}, respectively.

To match the surface tension of the sharp interface model, α must satisfy

$$\int_{-\infty}^{\infty} \epsilon \alpha |c_x^{eq}|^2 dx = 1, \tag{12}$$

where $c^{eq}(x, y) = \left[1 + \tanh \left(x / \left(2\sqrt{2}\epsilon \right) \right) \right] / 2$ is an equilibrium composition profile in the infinite domain when the chemical potential is given as Eq. (6) [17] and it is a good approximation in the finite domain. By using basic calculus, we get

$$\int_{-\infty}^{\infty} \epsilon \alpha |c_x^{eq}|^2 dx = \int_{-\infty}^{\infty} \frac{\alpha}{32\epsilon} \operatorname{sech}^4 \frac{x}{2\sqrt{2}\epsilon} dx = \frac{\alpha}{6\sqrt{2}}. \tag{13}$$

Therefore from Eqs. (12) and (13), we get $\alpha = 6\sqrt{2}$. For example, for two component immiscible fluids, $c_3 = c_4 = 0$ and $c_2 = 1 - c_1$. Let $c_1 = c$, then Eq. (11) reduces to $\mathbf{SF}(\mathbf{c}) = \sigma_{12} \mathbf{sf}(c) \delta(c, 1-c) = -\sigma_{12} \nabla \cdot (\nabla c / |\nabla c|) [5 \alpha \epsilon c (1-c) |\nabla c|^2] \nabla c / |\nabla c|$. Now we can consider the term, $5\alpha\epsilon c(1-c)|\nabla c|^2$, as our new smoothed Dirac delta function, i.e.,

$$\int_{-\infty}^{\infty} 5 \alpha \epsilon c (1-c) |\nabla c|^2 dx = 1. \tag{14}$$

In Fig. 4, the dotted line is concentration field $c = 0.5(1 + \tanh(x / \left(2\sqrt{2}\epsilon \right)))$, the dashed line is $5c(1-c)$, the dash-dot line is the Dirac delta function $\alpha \epsilon c_x^2$ in [18], and the solid line is the new Dirac delta function, $5\alpha\epsilon c(1-c)c_x^2$. We set $\epsilon = 0.1$.

We note that the new smoothed Dirac delta function, $5\alpha\epsilon c(1-c)|\nabla c|^2$, allows us to model any number of multi-compo-

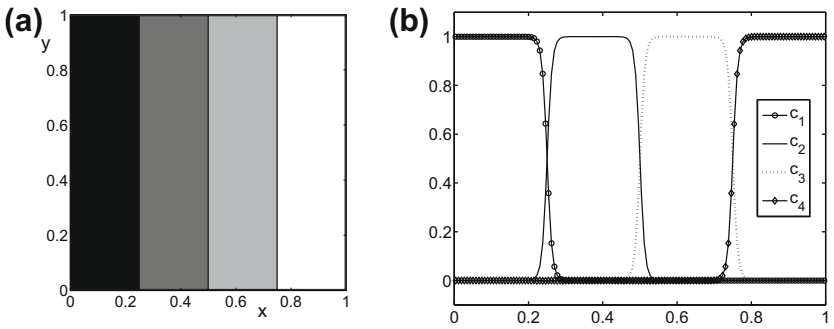

Fig. 3. (a) The initial configuration. (b) Vertical cutline of phase fields at $y = 0.5$.

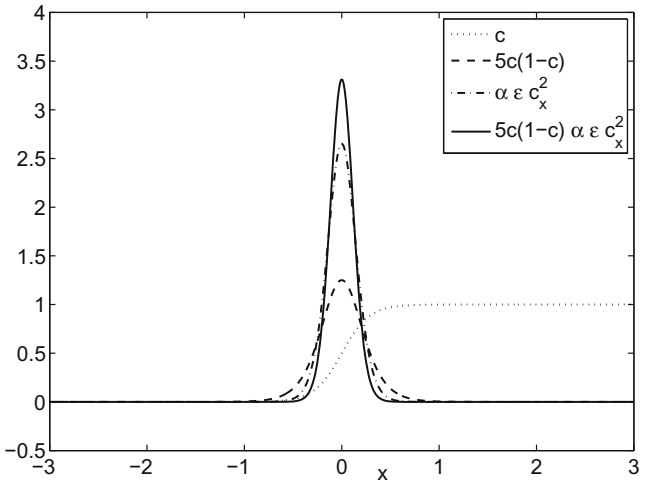

Fig. 4. The dotted line represents concentration field $c = 0.5(1 + \tanh(x/(2\sqrt{2}\epsilon)))$; the dashed line is $5c(1-c)$; the dash-dot line is the Dirac delta function $\alpha\epsilon c_x^2$ in [18]; and the solid line is the new Dirac delta function, $5\alpha\epsilon c(1-c)c_x^2$. We took $\alpha = 6\sqrt{2}$ and $\epsilon = 0.1$.

nent (more than three) fluid flows. In general, for the interface between fluid i and fluid j, we have

$$\int_{-\infty}^{\infty} 15\sqrt{2}\epsilon c_i c_j(|\nabla c_i|^2 + |\nabla c_j|^2)dx = 1, \tag{15}$$

where the integration is taken across the interface.

2.2. Nondimensional governing equations

To make the governing equations dimensionless, we choose the following definitions

$$\mathbf{x}' = \frac{1}{L}\mathbf{x}, \quad \mathbf{u}' = \frac{1}{U}\mathbf{u}, \quad t' = \frac{U}{L}t, \quad \rho' = \frac{\rho}{\rho_1}, \quad p' = \frac{p}{\rho_1 U^2}, \quad \eta' = \frac{\eta}{\eta_1},$$

where the primed quantities are dimensionless and L, U, ρ_1, and η_1 are, respectively, the characteristic length, characteristic velocity, the density of fluid 1, and the dynamic viscosity of fluid 1. Substituting the above into Eqs. (7)–(10), and dropping the primes, we have the following nondimensional system:

$$\frac{\partial \mathbf{u}}{\partial t} + \mathbf{u}\cdot\nabla\mathbf{u} = -\nabla p + \frac{1}{Re}\nabla\cdot[\eta(\mathbf{c})(\nabla\mathbf{u} + \nabla\mathbf{u}^T)] + \mathbf{SF}, \tag{16}$$

$$\nabla\cdot\mathbf{u} = 0, \tag{17}$$

$$\frac{\partial \mathbf{c}}{\partial t} + \mathbf{u}\cdot\nabla\mathbf{c} = \frac{1}{Pe}\Delta\boldsymbol{\mu}, \tag{18}$$

$$\boldsymbol{\mu} = \mathbf{f}(\mathbf{c}) - \epsilon^2\Delta\mathbf{c}, \tag{19}$$

where $\mathbf{f}(\mathbf{c})$ and ϵ are redefined according to the scaling and

$$\mathbf{SF}(\mathbf{c}) = \sum_{i=1}^{3}\left(\sum_{j=i+1}^{4}\frac{\delta(c_i,c_j)}{2We_{ij}}[\mathbf{sf}(c_i) + \mathbf{sf}(c_j)]\right). \tag{20}$$

The dimensionless parameters are the Reynolds number, $Re = \rho_1 UL/\eta_1$, the Weber number, $We_{ij} = \rho_1 LU^2/\sigma_{ij}$, and the diffusional Peclet number, $Pe = LU/(M\mu_*)$. Here μ_* denotes a characteristic scale involving both an anti-diffusive Laplacian and a diffusive bi-Laplacian in $\boldsymbol{\mu}$.

3. Numerical solution

A staggered marker-and-cell (MAC) mesh of Harlow and Welch [16] is used in which pressure and phase fields are stored at cell centers and velocities at cell interfaces. Let h be a mesh size. The center of each cell, Ω_{ij}, is located at $(x_i, y_j) = ((i-0.5)h, (j-0.5)h)$ for $i = 1,\ldots,M$ and $j = 1,\ldots,N$. M and N are the numbers of cells in x and y-directions, respectively. The cell vertices are located at $\left(x_{i+\frac{1}{2}}, y_{j+\frac{1}{2}}\right) = (ih, jh)$. At the beginning of each time step, given $\mathbf{u}^n$, and $\mathbf{c}^n$, we want to find $\mathbf{u}^{n+1}, \mathbf{c}^{n+1}$, and p^{n+1} which solve the following temporal discretization of the Eqs. (16)–(19) of motion:

$$\frac{\mathbf{u}^{n+1} - \mathbf{u}^n}{\Delta t} = -\nabla_d p^{n+1} + \frac{1}{Re}\nabla_d\cdot\eta(\mathbf{c}^n)[\nabla_d\mathbf{u}^n + (\nabla_d\mathbf{u}^n)^T] + \mathbf{SF}^n - (\mathbf{u}\cdot\nabla_d\mathbf{u})^n, \tag{21}$$

$$\nabla_d\cdot\mathbf{u}^{n+1} = 0, \tag{22}$$

$$\frac{\mathbf{c}^{n+1} - \mathbf{c}^n}{\Delta t} = \frac{1}{Pe}\Delta_d\boldsymbol{\mu}^{n+\frac{1}{2}} - (\mathbf{u}\cdot\nabla_d\mathbf{c})^n, \tag{23}$$

$$\boldsymbol{\mu}^{n+\frac{1}{2}} = \frac{1}{2}[\mathbf{f}(\mathbf{c}^n) + \mathbf{f}(\mathbf{c}^{n+1})] - \frac{1}{2}\epsilon^2\Delta_d(\mathbf{c}^n + \mathbf{c}^{n+1}). \tag{24}$$

For details of the numerical solution using a projection method and a nonlinear multigrid method, we refer to [19].

4. Computational verification of the model

We now present the numerical results for several standard problems with four component mixtures to illustrate the robustness and to test accuracy of the new phase-field model for multicomponent immiscible fluid flows. The numerical experiments are the phase separations via spinodal decomposition in a quaternary mixture with different average compositions, the pressure field distribution, and the dynamics of two droplets inside another drop embedded in the ambient liquid.

4.1. Spinodal decomposition – phase separation of a four-component mixture

We began the numerical experiments with an example of the spinodal decomposition of a quaternary mixture with components A, B, C, and D of the local mass fractions c_1, c_2, c_3, and c_4, respectively. We used the quaternary Cahn–Hilliard system, (9) and (10) with the zero velocity, $\mathbf{u} = \mathbf{0}$. In this experiment, we ignore the hydrodynamic effects. In the simulations, the initial conditions were random perturbations of the maximum amplitude 0.05 of the uniform state $\mathbf{c}_{ave} := \left(\frac{1}{|\Omega|}\int_\Omega c_1 d\mathbf{x}, \frac{1}{|\Omega|}\int_\Omega c_2 d\mathbf{x}, \frac{1}{|\Omega|}\int_\Omega c_3 d\mathbf{x}\right)$. We took $\epsilon = 0.008$. A 256×256 mesh was used on the square domain $\Omega = [0,8]\times[0,8]$ for the spatial discretization and a time step, $\Delta t = 0.1/256$ was employed for the time integration.

In the first experiment, the initial conditions were random perturbations of the uniform state $\mathbf{c}_{ave} = (1/4, 1/4, 1/4)$. The morphological evolution predicted from the numerical simulation is exhibited in Fig. 5a. The area shown by white indicates the D phase region, while the gray, dark gray, and black color regions stand for A-rich, B-rich and C-rich domains, respectively. Since the composition is completely symmetric with respect to the four components, all four phases have similar morphologies and evolution dynamics [7].

In the second experiment with $\mathbf{c}_{ave} = (1/5, 1/5, 1/5)$, Fig. 5b shows the time evolution of the quaternary mixture system. We observed four phases in the early stages of spinodal decomposition. As shown for time $t = 0.0977, c_1 + c_2 + c_3$, and c_4 phases appear as interconnected at the initial stages of decomposition which is very similar to that observed in binary systems. In the third experiment with $\mathbf{c}_{ave} = (1/6, 1/6, 1/6)$ (Fig. 5c), initially, we see four phases, one of them dominated by c_4. The evolution of the system is in the direction $c_1 + c_2 + c_3$ and c_4.

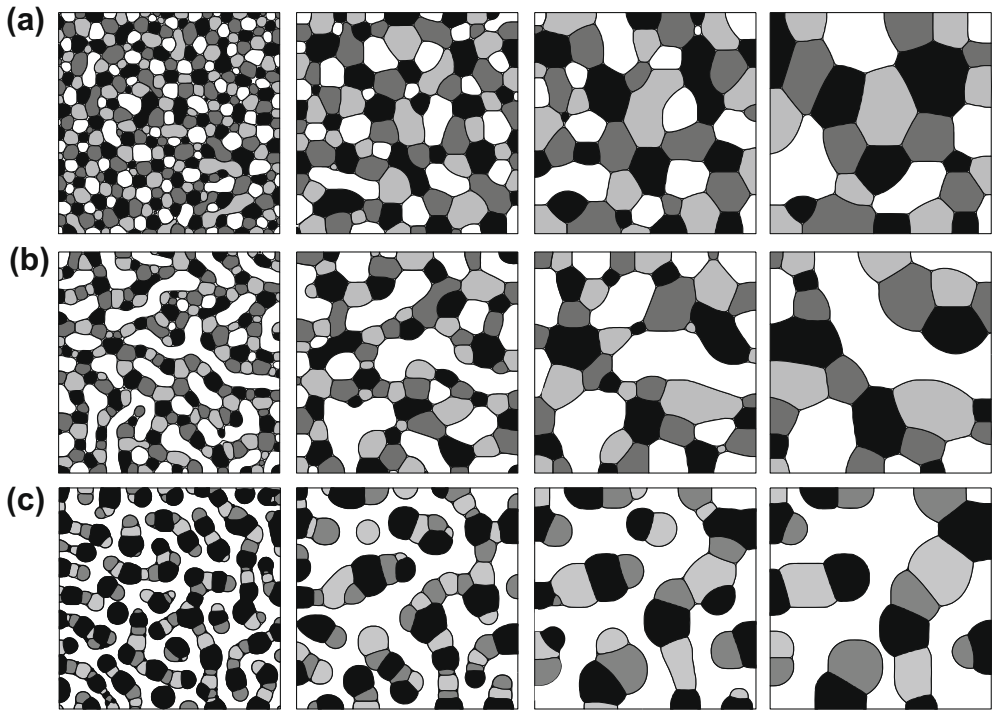

Fig. 5. Temporal evolution of morphologies during a spinodal phase separation of a quaternary mixture system with three different values of the average composition (a) $\mathbf{c}_{ave} = (1/4, 1/4, 1/4)$, (b) $\mathbf{c}_{ave} = (1/5, 1/5, 1/5)$, and (c) $\mathbf{c}_{ave} = (1/6, 1/6, 1/6)$, respectively. The times are $t = 0.0977, 0.3418, 0.7324$, and 1.9531 (left to right). Phase A is represented by the gray region, phase B by the dark gray region, phase C by the black region, and phase D by the white region.

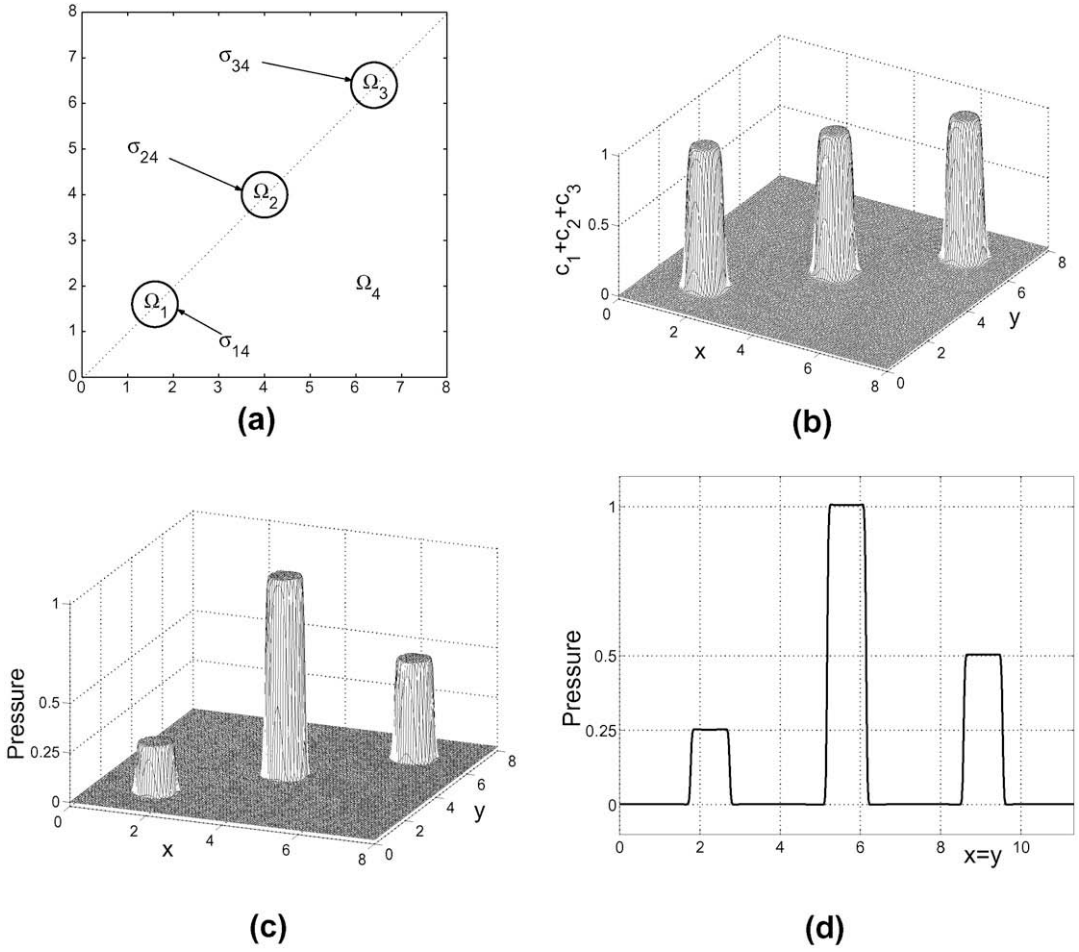

Fig. 6. (a) A schematic of two-dimensional three drops. (b) The sum of the concentration fields – $c_1 + c_2 + c_3$. (c) The pressure field. (d) A slice plot of the pressure field on $y = x$ (dotted line in (a)).

4.2. The pressure field distribution for three stationary drops

To demonstrate the ability to calculate the pressure field directly from the governing equations using the present model, we considered the equilibrium of three drops placed within another fluid. In the absence of viscous, gravitational, and other external forces, surface tension caused a static liquid drop to become spherical. The Laplace formula [4,23] for an infinite cylinder surrounded by a background fluid at zero pressure gives

$$p_{\text{drop}} = \sigma_{ij}\kappa = \frac{\sigma_{ij}}{R}, \tag{25}$$

where p_{drop} is the pressure of a droplet of radius R, σ_{ij} is the surface tension coefficient between fluid i and fluid j, and κ is the mean curvature. The initial conditions (see Fig. 6a and b) were

$$c_1(x,y,0) = 0.5\left(1-\tanh\left[\left(\sqrt{(x-1.6)^2+(y-1.6)^2}-0.5\right)\Big/2\sqrt{2}\epsilon\right]\right),$$
$$c_2(x,y,0) = 0.5\left(1-\tanh\left[\left(\sqrt{(x-4)^2+(y-4)^2}-0.5\right)\Big/2\sqrt{2}\epsilon\right]\right),$$
$$c_3(x,y,0) = 0.5\left(1-\tanh\left[\left(\sqrt{(x-6.4)^2+(y-6.4)^2}-0.5\right)\Big/2\sqrt{2}\epsilon\right)\right).$$

We solved the following Eq. (26) on the computational domain, $\Omega = [0,8]\times[0,8]$ with a uniform grid of 512×512. The drop radius $R = 0.5, \sigma_{14} = 1, \sigma_{24} = 4, \sigma_{34} = 2$, and $\sigma_{12} = \sigma_{13} = \sigma_{23} = 1$.

$$\Delta p = \nabla\cdot\mathbf{SF}. \tag{26}$$

In Fig. 6c, the pressure field is shown for three drops. Fig. 6d shows that the pressure jumps along the line, $x = y$, calculated from our model obeying Laplace law.

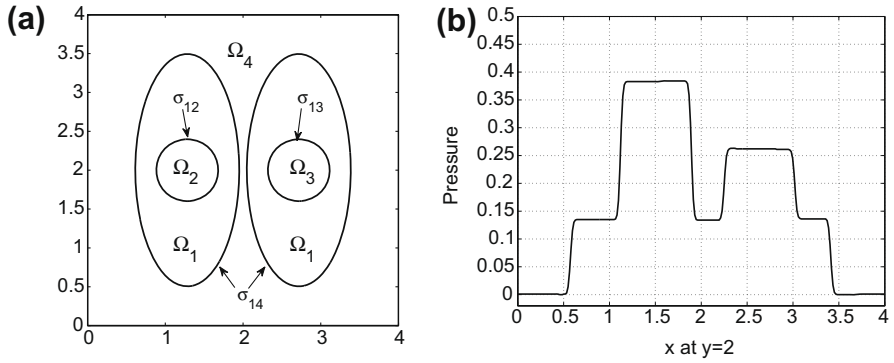

Fig. 7. (a) Schematic (b) A slice plot of the pressure field on $y = 2$.

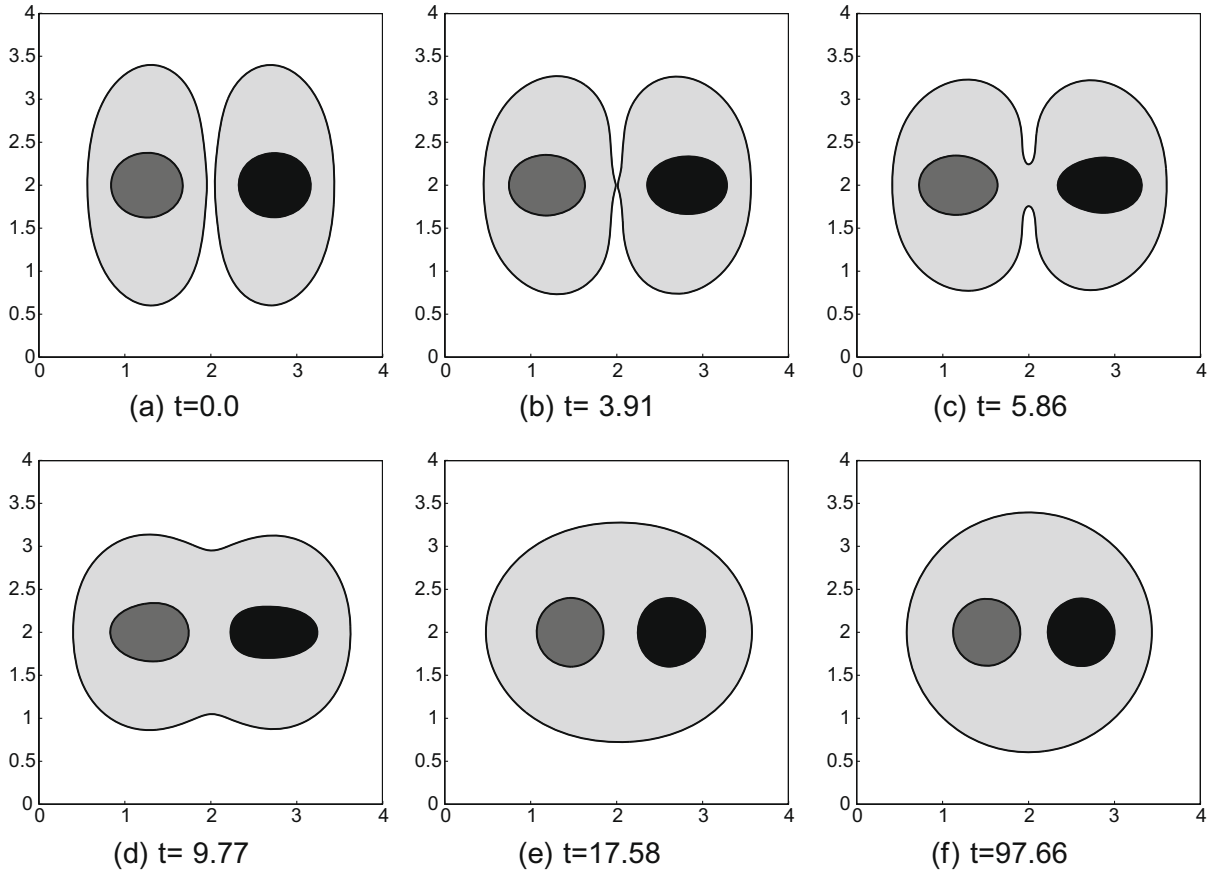

Fig. 8. Temporal evolution. Fluid Ω_1 is represented by the gray region; fluid Ω_2 by the dark gray region; fluid Ω_3, by the black region; and fluid Ω_4, by the white region.

4.3. Topological transition and the dynamics of droplets

We consider the dynamics of two droplets inside other elliptical drops embedded in the ambient liquid. The initial condition is that of two droplets, Ω_2 and Ω_3, enclosed by elliptical drops, Ω_1, which are also in the ambient fluid, Ω_4 (see Fig. 7a). The initial velocity is zero, i.e.,

$$c_1(x,y,0) = 1 - \frac{1}{2}\tanh\frac{\sqrt{5(x-1.28)^2+(y-2)^2}-1.5}{2\sqrt{2}\epsilon} - \frac{1}{2} \times \tanh\frac{\sqrt{5(x-2.72)^2+(y-2)^2}-1.5}{2\sqrt{2}\epsilon} - c_2(x,y,0) - c_3(x,y,0),$$

$$c_2(x,y,0) = \frac{1}{2}\left(1-\tanh\frac{\sqrt{(x-1.28)^2+(y-2)^2}-r}{2\sqrt{2}\epsilon}\right),$$

$$c_3(x,y,0) = \frac{1}{2}\left(1-\tanh\frac{\sqrt{(x-2.72)^2+(y-2)^2}-r}{2\sqrt{2}\epsilon}\right),$$

$$u(x,y,0) = v(x,y,0) = 0,$$

where $r = 0.4$ is the radius of the drops. We solved Eqs. (16)–(19) on the computational domain, $\Omega = [0,4]\times[0,4]$ with a uniform grid of 256×256, time step, $\Delta t = 0.05/256$, and $\epsilon = 0.015$. Periodic boundary conditions for both directions are applied. We take the viscosities of the components to be matched and the following parameters.
$We_{14} = We_{23} = We_{24} = We_{34} = 5, We_{12} = 10, We_{13} = 20, Re = 5$, and $Pe = 1/\epsilon$.

We show in Fig. 8a–f the temporal evolution of the dynamics of two droplets inside other elliptical drops embedded in the ambient liquid. The driving force for the flow is surface tension. Fluid Ω_1 is represented by the gray region; fluid Ω_2, by the dark gray region; fluid Ω_3 by the black region; and fluid Ω_4, by the white region. Initially the elliptical drops deform to reduce the higher curvature; then, coalescence occurs around $t = 3.91$. Eventually, at later times, all interface shapes became an equilibrium circular shape (see Fig. 8f), Fig. 7b shows the pressure distribution at $y = 2$. According to Laplace formula, (25), the theoretical drop pressure jumps across the circles:.

$$[p]_{\Gamma_{12}} = \frac{1}{rWe_{12}} = 0.25,$$
$$[p]_{\Gamma_{13}} = \frac{1}{rWe_{13}} = 0.125,$$
$$[p]_{\Gamma_{14}} = \frac{1}{RWe_{14}} = 0.1416,$$

where $R = 1.4127$ is the measured radius of the largest circle in Fig. 8f. The numerical values of the pressure jump across the drops are $[p]^{num}_{\Gamma_{12}} = 0.248, [p]^{num}_{\Gamma_{13}} = 0.126$, and $[p]^{num}_{\Gamma_{14}} = 0.135$. These values show how well the pressure field fulfilled Laplace law, (25).

5. Conclusions

We proposed the generalized continuous surface tension force (GCSF) model for surface tension for multi-component fluid flow. In the GCSF model, a surface force was formulated to model numerically the surface tension effects at fluid interfaces having finite thickness. The method is ideally suited for multi-component fluid flows. We overcame previous shortcomings on the extension to multi-component (more than three) fluid flows. The GCSF model has been validated successfully on both static and dynamic interfaces having surface tension. An important aspect of the GCSF is its generality with respect to the number of the fluid components. In general, for N component fluids, the surface tension force formulation is

$$\mathbf{SF}(\mathbf{c}) = \sum_{i=1}^{N-1}\left(\sum_{j=i+1}^{N}\frac{\sigma_{ij}}{2}[\mathbf{sf}(c_i)+\mathbf{sf}(c_j)]\delta(c_i,c_j)\right).$$

Although this generalized surface tension force formulation was described in the context of the phase-field method, we expect that it can be useful in other methods such as the level set method. Further topics of our future research related to the presented GCSF include higher order numerical treatments and sophisticated formula to accurately recover the interfacial angles at triple points where three fluids are in contact. Also, to speed up the calculations, we will investigate an adaptive time stepping algorithm as in [10].

Acknowledgement

This work was supported by the Korea Science and Engineering Foundation (KOSEF) grant funded by the Korea government (MEST) (No. R01-2008-000-20855-0). The author thanks Professors Kyungkeun Kang and Jihoon Lee for valuable discussions on this topic. The author also thanks an anonymous referee for very valuable comments and suggestions on this paper.

References

[1] D.M. Anderson, G.B. McFadden, A.A. Wheeler, Diffuse-interface methods in fluid mechanics, Annu. Rev. Fluid Mech. 30 (1998) 139–165.
[2] V.E. Badalassi, H.D. Ceniceros, S. Banerjee, Computation of multiphase systems with phase field models, J. Comput. Phys. 190 (2003) 371–397.
[3] F. Boyer, C. Lapuerta, Study of a three component Cahn–Hilliard flow model, M2AN 40 (2006) 653–687.
[4] J.U. Brackbill, D.B. Kothe, C. Zemach, A continuum method for modeling surface tension, J. Comput. Phys. 100 (1992) 335–354.
[5] Y.C. Chang, T.Y. Hou, B. Merriman, S. Osher, A level set formulation of Eulerian interface capturing methods for incompressible fluid flows, J. Comput. Phys. 124 (1996) 449–464.
[6] R. Chella, J. Viñals, Mixing of a two-phase fluid by cavity flow, Phys. Rev. E 53 (1996) 3832–3840.
[7] L.Q. Chen, A computer simulation technique for spinodal decomposition and ordering in ternary systems, Scr. Metall. Mater. 29 (1993) 683–688.
[8] C.M. Elliott, S. Luckhaus, A generalised diffusion equation for phase separation of a multi-component mixture with interfacial free energy, IMA Preprint Series 887, 1991.
[9] D.J. Eyre, Systems of Cahn–Hilliard equations, SIAM J. Appl. Math. 53 (1993) 1686–1712.
[10] H. Gomez, V.M. Calo, Y. Bazilevs, T.J.R. Hughes, Isogeometric analysis of the Cahn–Hilliard phase-field model, Comput. Meth. Appl. Mech. Engrg. 197 (2008) 4333–4352.
[11] D. Gao, N.B. Morley, V. Dhir, Numerical simulation of wavy falling film flow using VOF method, J. Comput. Phys. 192 (2003) 624–642.
[12] H. Garcke, B. Nestler, B. Stoth, On anisotropic order parameter models for multi-phase systems and their sharp interface limits, Physica D 115 (1998) 87–108.
[13] H. Garcke, B. Nestler, B. Stoth, A multi phase field: numerical simulations of moving phase boundaries and multiple junctions, SIAM J. Appl. Math. 60 (1999) 295–315.
[14] D. Gueyffier, J. Li, A. Nadim, R. Scardovelli, S. Zaleski, Volume-of-fluid interface tracking with smoothed surface stress methods for three-dimensional flows, J. Comput. Phys. 152 (1999) 423–456.
[15] C. Galusinski, P. Vigneaux, On stability condition for bifluid flows with surface tension: application to microfluidics, J. Comput. Phys. 227 (2008) 6140–6164.
[16] F.H. Harlow, J.E. Welch, Numerical calculation of time-dependent viscous incompressible flow of fluid with free surface, Phys. Fluids 8 (1965) 2182–2189.
[17] D. Jacqmin, Contact-line dynamics of a diffuse fluid interface, J. Fluid Mech. 402 (2000) 57–88.
[18] J.S. Kim, A continuous surface tension force formulation for diffuse-interface models, J. Comput. Phys. 204 (2005) 784–804.
[19] J.S. Kim, Phase field computations for ternary fluid flows, Comput. Meth. Appl. Mech. Engrg. 196 (2007) 4779–4788.
[20] J.S. Kim, K. Kang, J.S. Lowengrub, Conservative multigrid methods for ternary Cahn–Hilliard systems, Commun. Math. Sci. 2 (2004) 53–77.
[21] J.S. Kim, J.S. Lowengrub, Phase field modeling and simulation of three-phase flows, Interfaces Free Bound. 7 (2005) 435–466.

[22] J.S. Kim, J.S. Lowengrub, Interfaces and multicomponent fluids, Encyclopedia of Mathematical Physics, Elsevier, 2006.
[23] L.D. Landau, E.M. Lifshitz, Fluid Mechanics, Pergamon Press, Oxford, 1987.
[24] L. Lee, R.J. LeVeque, An immersed interface method for incompressible Navier–Stokes equations, SIAM J. Sci. Comput. 25 (2003) 832–856.
[25] C. Liu, J. Shen, A phase field model for the mixture of two incompressible fluids and its approximation by a Fourier-spectral method, Physica D 179 (2003) 211–228.
[26] M. De Menech, Modeling of droplet breakup in a microfluidic T-shaped junction with a phase-field model, Phys. Rev. E 73 (2006) 031505-1–031505-9.
[27] L.M. Deremble, P. Tabeling, Droplet breakup in microfluidic junctions of arbitrary angles, Phys. Rev. E 74 (2006) 035303-1–035303-4.
[28] M. Nelleon, Mechanics and Properties of Matter, Heineman, London, 1952.
[29] S. Osher, J.A. Sethian, Fronts propagating with curvature-dependent speed: algorithms based on Hamilton–Jacobi formulations, J. Comput. Phys. 79 (1988) 1–49.
[30] D.A. Porter, K.E. Easterling, Phase Transformations in Metals and Alloys, van Nostrand Reinhold, 1993.
[31] E.G. Puckett, A.S. Almgren, J.B. Bell, D.L. Marcus, W.J. Rider, A high-order projection method for tracking fluid interfaces in variable density incompressible flows, J. Comput. Phys. 130 (1997) 269–282.
[32] Y. Renardy, M. Renardy, PROST: A parabolic reconstruction of surface tension for the volume-of-fluid method, J. Comput. Phys. 183 (2002) 400–421.
[33] Y. Renardy, M. Renardy, V. Cristini, A new volume-of-fluid formation for surfactants and simulations of drop deformation under shear at a low viscosity ratio, Eur. J. Mech. B/Fluids 21 (2002) 49–59.
[34] J.A. Sethian, Theory, algorithms, and applications of level set methods for propagating interfaces, Acta Numer. (1996) 309–395.
[35] J.A. Sethian, Level Set Methods: Evolving Interfaces in Geometry, Fluid Mechanics, Computer Vision and Material Sciences, Cambridge University Press, Cambridge, UK, 1996.
[36] K.A. Smith, F.J. Solis, D.L. Chopp, A projection method for motion of triple junctions by levels sets, Interfaces Free Bound. 4 (2002) 263–276.
[37] H. Tang, L.C. Wrobel, Z. Fan, Tracking of immiscible interfaces in multiple-material mixing processes, Comp. Mater. Sci. 29 (2004) 103–118.
[38] G. Tryggvason, B. Bunner, A. Esmaeeli, D. Juric, N. Al-Rawahi, W. Tauber, J. Han, S. Nas, Y.J. Jan, A front-tracking method for the computations of multiphase flow, J. Comput. Phys. 169 (2001) 708–759.
[39] H.S. Udaykumar, H.C. Kan, W. Shyy, R. Tran-Son-Tay, Multiphase dynamics in arbitrary geometries on fixed cartesian grids, J. Comput. Phys. 137 (1997) 366–405.
[40] P. Yue, J.J. Feng, C. Liu, J. Shen, A diffuse-interface method for simulating two-phase flows of complex fluids, J. Fluid Mech. 515 (2004) 293–317.